Experimental and Numerical Analysis of Heat, Air, and Moisture Transfer in a Lightweight Building Wall

Tadiwos Zerihun Desta, PhD **Staf Roels, PhD**

ABSTRACT

This paper reports on experimental and numerical studies on heat, air, and moisture (HAM) transfer through a full-scale lightweight building envelope wall. The wall is a multilayered structure built up from outside to inside of external board, vented cavity, fiberboard sheathing, mineral wool between wooden studs, and interior finishing. The global wall has a surface area of 1.80 × 2.60 m^2 and is subdivided into three vertical parts. The parts differ from each other by the applied interior finishing. The first part is finished with a wooden interior finishing, which is rather vapor tight. The second part is finished with uncoated gypsum board (airtight but vapor open), and the third part has an air and vapor barrier, an air gap, and interior gypsum board finishing. The latter can be seen as an air- and vapor-tight reference case. Between the different layers of each part and on the surfaces of the wall, humidity, temperature, and heat flux sensors are placed in a three-dimensional matrix. The fiberboard sheathing contains nine removable specimens. By regularly weighing the sheathing samples, their moisture content can be quantified. The collected data are used to investigate the hygrothermal behavior of the wall. Moreover, the experimental data are compared with results from a Glaser calculation and a numerical HAM simulation.

The obtained results show that the amount of moisture accumulation in the exterior sheathing is influenced by vapor permeability of the interior finishing as long as the walls are airtight. As soon as the interior finishing is made air open, convective driven vapor flow becomes the dominant process, increasing the amount of moisture accumulation drastically.

INTRODUCTION

Due to the growing concern in the building sector to reduce energy consumption and the emission of greenhouse gasses, lightweight building constructions are becoming more and more popular, even in countries with masonry traditions. The main reason is the simplicity to incorporate a thick insulation layer between the wooden studs, making lightweight buildings easy to build, sustainable, and renewable. Although such constructions reduce energy consumption significantly, the moisture intrusion tolerance for lightweight structures is low (Li et al. 2009). The most important moisture sources are wetting during the construction phase, rain leakage, and moisture accumulation due to vapor diffusion and convection.

To analyze the moisture response of building envelopes, several hygrothermal simulation tools have been developed in the last decades. These hygrothermal building envelope models—often referred to as *HAM models*—evolved from the Glaser method, a one-dimensional hand calculation method for vapor diffusion through insulated components (Glaser 1958; Vos and Coelman 1967; Hens 1975). Through the years, models that incorporate heat and moisture capacity; liquid water transport and air transport; and one- and two-dimensional aspects, accounting for different moisture sources such as wind driven rain, rising damp, initial moisture, and interstitial and surface condensation, have been developed (e.g., Pedersen [1990], Karagiozis [1993], Künzel [1994], and Grunewald [1997]). Several of these HAM models are nowadays commercially available for practitioners in the field and are increasingly used for analyzing the heat and moisture behavior of building components. Of course, the relevance of

Tadiwos Zerihun Desta *is a researcher and* ***Staf Roels*** *is a professor in the Division of Building Physics, Catholic University of Leuven, Leuven, Belgium.*

using HAM models as engineering tools strongly depends on the validity of the models and their capability to predict the real performance.

An important effort to standardize HAM modeling procedures was made by the EU-initiated HAMSTAD project (Heat, Air, and Moisture Standards Development) (Adan et al. 2004). Bench mark cases were used for model validation. The cases were selected in such a way that various materials, transport mechanisms, and climatic boundary conditions were covered (Hagentoft et al. 2004). The validation, though, relied only on intermodal comparison or on problems with simple analytic solutions since accurate and well-documented experimental data are scarce. In the framework of IEA ECBCS Annex 41 (Roels et al. 2009), a transient heat and moisture experiment on a porous building material was performed for benchmarking numerical models with respect to hygroscopic loading. These kinds of well-controlled laboratory experiments are an important part of validating HAM models, but of course the ultimate goal of hygrothermal building envelope models is to predict the heat, air, and moisture (HAM) response of real building components under real climatic conditions.

This paper describes a carefully planned full-scale experiment suitable for model validation. The test case is rather unique in its complexity, configuration, and follow-up. The experimental setup was a lightweight building envelope wall. The global wall was subdivided into three sections that differed in air- and vapor-tightness of the interior finishing. The sections were exposed to identical outside and inside conditions, which makes it possible to compare the dynamic hygric behavior between the three configurations. The experiment ran for almost two years. During this time, the air pressure difference across the wall and the temperatures, humidities, and heat fluxes within the construction were continuously logged. In addition, the evolution of the moisture content of the fiberboard sheathing was quantified by regularly weighing nine removable specimens of the board.

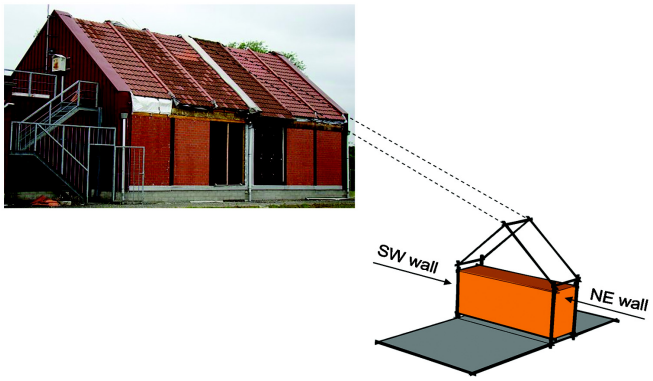

Figure 1 *The VLIET test building at K.U.Leuven, Belgium, and the schematic view of the compartment with the test wall in the NE façade.*

The first part of this paper describes the experimental setup. Then the measured data are presented and analyzed. Finally, the measurement results are compared with some preliminary numerical simulations.

EXPERIMENTAL SETUP

Test Setup

The experimental setup is situated in the VLIET test building, located at K.U.Leuven, Belgium (50.88°N, 4.7°E). The test building itself was constructed for the comprehensive study of the hygrothermal behavior of building components under real climatic conditions (Roels and Deurinck 2010). In the building, a compartment has been isolated connecting the southwest (SW) and northeast (NE) façades (Figure 1). The room has a length of 6.5 m, a width of 1.8 m, and a height of 2.6 m. Except the test wall in the NE façade all other walls, the roof and floor are made air- and vapor-tight by using plywood in combination with polyethylene plastic foil.

The test wall at the NE side is a lightweight wooden construction. The global wall has a surface area of 1.80 × 2.60 m^2 and is subdivided into three vertical sections, each with a similar configuration but with different characteristics for the heat, air, and vapor transport.

The basic configuration of all three sections consists of wooden studs (25 × 200 mm) with mineral wool insulation (200 mm) in between. At the outside, this load-bearing construction is finished with a fiberboard sheathing (18 mm), followed by a cavity (25 mm) and water-resistant wooden multiplex board (18 mm). The cavity is ventilated naturally through openings at the top and bottom of the outer board (Figure 2). Thus far, the three parts of the wall (i.e., left,

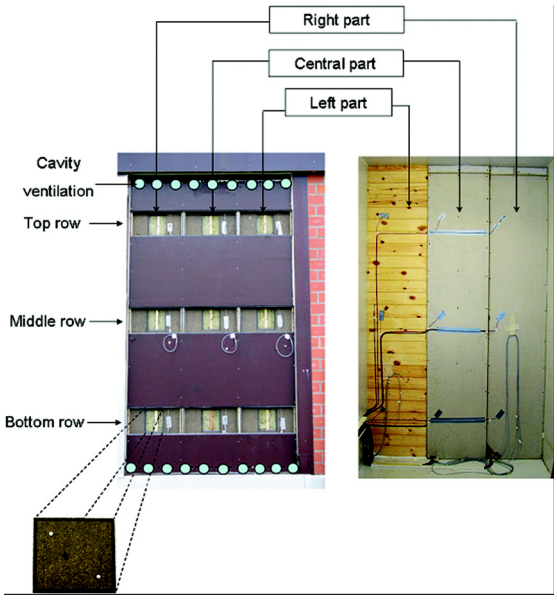

Figure 2 *Outside view (left) and inside view (right) of the test wall.*

middle, and right parts) are identical. The interior finishing, however, varies. The left part is finished with a wooden interior finishing (12.5 mm), which is relatively air open. It will be referred to as the *wooden section*. The right part has an uncoated gypsum board (12.5 mm) that is airtight but vapor open as an interior finishing. This part will be referred to as the *gypsum section*. The middle part has a polyethylene air and vapor barrier (0.2 mm), an unventilated cavity (25 mm), and interior uncoated gypsum board finishing (12.5 mm). The latter can be seen as an air- and vapor-tight reference case (see Figure 4) and will be identified as the *reference section*.

The choice of the sheathing follows from the fact that the bituminous mixed wood fiberboard is very hygroscopic and allows capillary water transport. As a result, it can buffer large amounts of moisture and avoids in this way drainage of eventual moisture accumulation in the winter seasons. The fiberboard sheathing was constructed in such a way that each part of the wall contained three removable specimens of the board (Figure 2). The specimens are used to quantify the moisture evolution of the fiberboard sheathing in time. The weight increases/decreases of the boards have been measured on a regular basis.

The experiment ran from October 1, 2008, until April 30, 2010. During this period, the setup was adapted three times in order to study the effect of several internal and external conditions on the prevailing HAM transport. The first modification of the test configuration was performed on November 20, 2008, by introducing a moisture source in the room and controlling the room temperature at 20°C. The changes made the test configuration a representative dwelling room. After about three months of data collection, on March 5, 2009, a ventilation system (Figure 3) was introduced in order to study the effect of air transport on the hygrothermal performance of the building wall. In this stage, measurement of inlet air velocity together with the pressure drop across the NE wall was started. The ventilation system created a rather constant overpressure in the room, increasing the pressure drop over the NE test wall. However, significant airflow through the wall could not be attained due to the low air permeance of all sections of the wall. Finally, about seven months after the ventilation system was activated, on October 11, 2009, the interior finish-

Figure 3 *The ventilation system that penetrates through the SW wall.*

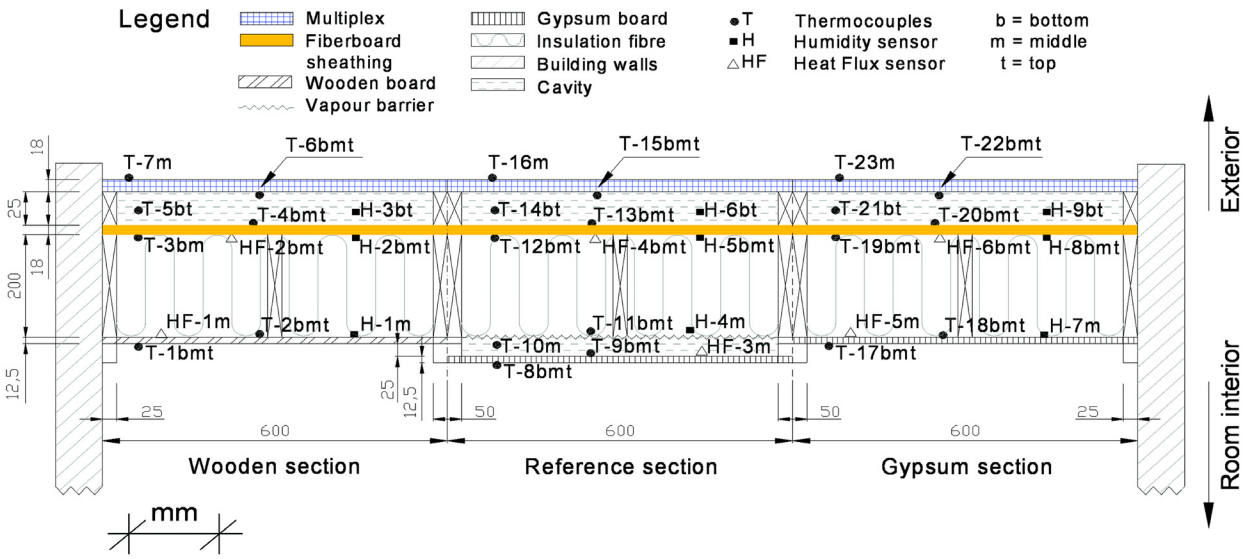

Figure 4 *Global configurations and positioning of the sensors inside and on the surface of the test wall. Left part: wooden section; middle part: reference section; right part: gypsum section.*

ing of the wooden section of the wall was made more air open to investigate the effect of increasing airflow rate on the hygroscopic response of the wall. Increasing the air permeance of the wooden finishing was achieved by drilling very small holes (1 mm in diameter) in an equidistant fine grid (50×50 mm^2).

The ventilation system, shown in Figure 3, consists of a small fan with a constant revolution rate and a polyethylene tube. The ventilation tube is extended into the room so that the airflow in the tube becomes fully developed before it is supplied to the room, avoiding abrupt airflow rate and pressure fluctuations in the room.

On the surfaces and within the test wall, a total of fifty seven thermocouples, eighteen humidity sensors, and twelve heat flux sensors were mounted in a structured manner (Figure 4). The sensors were placed in three rows—top (t), middle (m), and bottom (b)—covering the most important positions of the wall. In the room, nine thermocouples and three relative humidity sensors were hung on a grid. The pressure drops across the NE and SW walls together with the ventilation flow rates were measured. Outside conditions were logged with a weather station and meteorological mast (Abuku et al. 2009)

Table 1 summarizes the accuracy and other relevant information of the used sensors and other measuring instruments.

One of the key requirements for successful validation operation of numerical predictions is the availability of correct material properties (Roels et al. 2009). Therefore, all the essential hygrothermal properties of the applied materials were measured except that of the mineral wool, which was taken from Kumaran's (1996) work. For each property measurement, three samples were measured and mean values are reported hereafter.

MATERIAL PROPERTIES MEASUREMENT

Heat Transfer Properties

The thermal resistances of the building components are measured at temperatures ranging between 5°C and 40°C with the heat flow meter apparatus as described in the standard guidelines (ISO 1991). Table 2 provides the data at 20°C.

The heat capacity and density of all the materials shown in Table 2 are taken from the literature (Kumaran 1996) and product manuals of the suppliers.

Hygric Properties

The moisture capacities of the building components are measured according to the guidelines described in *EN 12571* (ISO 2000). Table 2 summarizes the data at 30%, 75%, and 94% RH.

The determination of water vapor transmission properties of the building components was performed according to the international standard procedure at 23°C (ISO 2001). Table 2 gives the dry cup (30% RH) and wet cup (90% RH) values of the equivalent air layer thickness of the different materials.

Liquid water transport in the interior finishing and mineral wool is unlikely. Therefore, only the water transport parameters for the moisture buffering fiberboard sheathing were measured. The capillary moisture content, the water adsorption coefficient, and the vacuum saturation moisture content of the fiberboard sheathing were found to be 0.6 kg/kg, 0.0052 kg/m^2·s$^{0.5}$, and 3.7 kg/kg, respectively.

Table 1. Accuracy of Sensors and Measuring Instruments

Test Type	Instrument	Manufacturer	Model	Measurement Range	Accuracy
Full-scale experiment at the test building	Thermocouple (type T)	Thermo-electric, Belgium	P-26-TT-IEC	Max. 105°C	±0.1°C
	Relative humidity sensor	Honeywell, Belgium	HIH-4000	0%–100%	±0.5%
	Heat flux sensor	Hukseflux Thermal Sensors, The Netherlands	HFP01	2000 to 2000 W/m^2	±5% of readings
	Pressure sensor	Halstrup Walcher Gmbh, Germany	P92	0–25 Pa	±4% of readings
	Velocity sensor	TSI Incorporated, USA	Model 8475	0.05–2.5 m/s	±3% of readings
	Balance	Mettler Toledo, Switzerland	PB1502-L	0–1.51 kg	±0.01 g
Small-scale laboratory setup for material property measurement	Balance	Mettler Toledo, Switzerland	XS1003s	0–1.01 kg	±0.001 g
	Pressure sensor	Druck Limited, UK	H02964	0–4 bar	±0.08% of readings

Table 2. Overview of the Material Properties

Parameter	Fiberboard Sheathing (FS)	Mineral Wool (MW)	Vapor Retarder (VR)*	Gypsum Board (GB)	Wooden Finish (WF), Undrilled	Wooden Finish (WF), Drilled
d	0.018	0.2	0.0002	0.0125	0.015	0.015
ρ	274	20	1000	700	400	400
c_p	2068	840	1400	870	2000	2000
λ @ 20°C	0.0452	0.0380	0.15	0.1940	0.0938	0.0938
w @ 30% RH	0.0318	0.0018	—	0.0381	0.0468	0.0468
w @ 75% RH	0.0604	0.0037	—	0.0514	0.0986	0.0986
w @ 94% RH	0.1201	0.0078	—	0.0707	0.1917	0.1917
s_d @ 30% RH	0.1286	0.5123	60	0.1158	1.9200	0.3040
s_d @ 90% RH	0.0589	0.5123	60	0.0572	0.0889	0.0812
a	0.16	4.66	—	0.0022	0.02	0.47
b	1	0.92	—	0.97	0.89	0.84

* The vapor barrier, polyethylene foil, is an airtight material with very low hygroscopic potential.

Air Transport Properties

The air permeance of the test wall is determined by combining permeance measurements of its components in a small-scale laboratory setup (Figure 5). The laboratory setup is an airtight chamber in which one of the faces is designed to be perfectly sealed with the sample, from which the permeance is going to be measured. The experiment is performed by injecting compressed air with variable pressure into the chamber and simultaneously recording the corresponding pressure drop and airflow rate across the sample.

The measured values are fitted with the following equation:

$$g_{air} = k_{air}\Delta p, \text{ but } k_{air} = a\Delta p^{b-1} \Rightarrow g_{air} = a\Delta p^{b} \qquad (1)$$

Once a and b are calculated from the curve fit between the airflow rate and the pressure drop across the samples, the air permeances, k_{air}, of the building materials are calculated using Equation 1. The parameters a and b for the building components of the test wall are provided in Table 2.

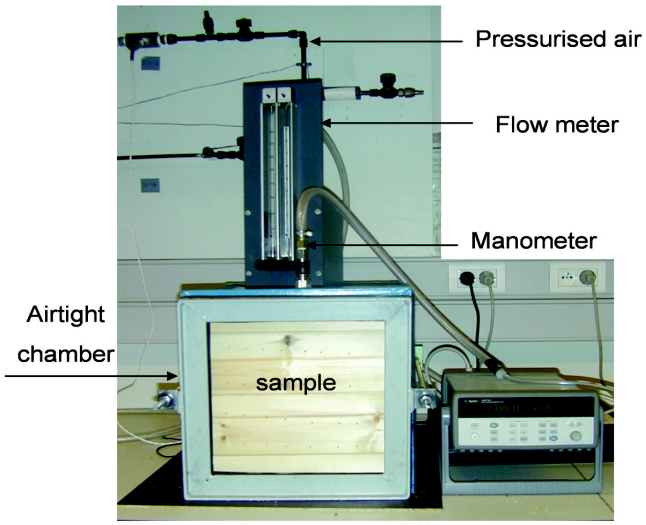

Figure 5 *Laboratory setup to determine the air permeance of building materials.*

MEASUREMENT RESULTS

The nine removable fiberboard sheathing specimens are weighed on a regular basis. Figure 6 shows the evolution of the moisture content of the specimens and the measured boundary conditions, i.e., indoor and outdoor cavity temperatures and vapor pressures together with the airflow rate through the wooden section of the wall. When comparing the first and second winters in this figure, the impact of the drilling of the wooden section on the hygrothermal behavior of this part is clearly visible.

When comparing the evolution of the moisture content of the fiberboard sheathing specimens, distinct different results are observed for the three wall compositions. The introduction of the moisture source on November 20, 2008, combined with the winter period, induced a moisture content rise in all specimens. The increase of the moisture content is, however, far more pronounced for the samples in the gypsum and wooden sections of the wall. The gypsum section, which is the most vapor open, shows in the first winter period the highest moisture increase. The increase in moisture content is very limited for the reference section because of the vapor barrier film. The ventilation system, installed on March 5, 2009, pressurized the room, and a slight increase in moisture content of the specimens was observed in the first winter immediately after activating the ventilation system.

After the first winter, all fiberboard sheathing specimens dried out again during summer 2009. The drilling of the wooden section on October 11, 2009, significantly increased the moisture transfer by both lowering the vapor resistance factor of the wall and enhancing the convective mass flow rate through the wall. As a result, the fiberboard sheathing specimens at the wooden section gained twice and four times as much moisture as those of the ones at the gypsum and reference sections, respectively (Figure 6).

The indoor humidity varied between 88.7% and 48.07% during the test period. Since there is no mechanical cooling in the test room, in summer 2009 the room temperature rose above the setpoint of 20°C. This rise in temperature, combined with the moisture source in the room, resulted in high indoor vapor pressure. However, in fall 2009 the effect of the drop in temperature and the drilling of the wooden section lowered the indoor vapor pressure significantly.

The top, middle, and bottom rows of the test configurations in the three parts of the wall showed different moisture content values. These may be attributed to circulation of air in the ventilated cavity at the outside of the wall and stack effect, resulting in disproportional moisture transport at the surfaces of the specimens situated at each row.

In Figure 6, the airflow through the wall is calculated by multiplying the pressure drop across the wall with the global air permeance of the wooden section of the wall. The air leakages through the gypsum and reference sections are considered to be negligible since the interior finishing of these parts of the wall (gypsum board and/or vapor barrier) are known to be airtight.

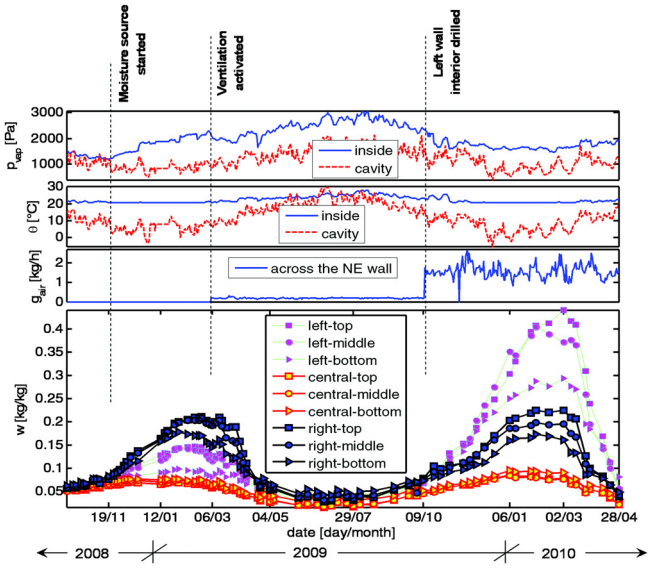

Figure 6 *Measurement results of inside and outside cavity vapor pressures, inside and outside cavity temperatures, airflow rates across the test wall, and moisture content evolutions of the nine removable fiberboard sheathing specimens.*

The air permeance of the wooden section (and hence of the global test wall) is calculated from the measured permeances of the building components at this section (Equation 1) by adding the airflow resistances (reciprocal of permeance) in series arrangement.

NUMERICAL SIMULATIONS

Both the Glaser method and a one-dimensional numerical model were used to simulate the combined heat and moisture transfer in the considered wall.

The Glaser Method

The Glaser method is an easy hand calculation tool to investigate the moisture performance of building envelopes with respect to interstitial condensation (CEN 2001). The method, however, is based on several assumptions, such as:

- the thermal and moisture transport are independent, one-dimensional and steady state;
- the moisture is transported only by vapor diffusion according to Fick's law;
- the heat flow is exclusively by conduction according to Fourier's law;
- there is no sorption or migration of water in the wall;
- liquid moisture in the wall is due to condensation of water vapor, which takes place on those positions where the water vapor pressure is greater than the saturated vapor pressure; and
- neither liquid transport nor air transport is considered.

Since the Glaser method is based on steady-state conditions, weekly average inside and outside conditions are used. The inside and outside boundary conditions are taken from data measured at the ventilated air cavity and in the room, respectively (see Figure 6 for the values). Since air transport is not included in the method, only the first year is considered (from mid October 2008 until the beginning of July 2009).

A typical Glaser diagram of a day when condensation occurs is shown in Figure 7.

According to the Glaser method, no interstitial condensation was predicted for the fiberboard sheathing specimens located in the wooden and reference sections of the wall. However, for specimens at the gypsum sections, interstitial condensation was predicted at the inside of the fiberboard sheathing. Figure 8 compares the measured and the Glaser predicted specimen moisture contents at the gypsum section. The amount of interstitial condensation increased until the end of February 2009. Afterwards, the accumulated interstitial condensation evaporated and finally a complete drying out was predicted for the middle of April 2009.

Modified Glaser Method

The modified version of the Glaser method combines both diffusion and convection of heat and moisture transfer through an air-permeable media. A full description of the

method can be found in the book by Hens (2007). Data measured from the end of October 2009 until the end of January 2010 at the ventilated air cavity (outside condition) and in the room (inside condition) are used (Figure 6). Similar to the Glaser method, weekly averaged data are used to comply with the steady-state assumption of the model. Since the reference and gypsum sections of the wall are kept airtight, only the heat and moisture transport in the wooden section of the wall is assessed using the model. The airflow rate in Figure 9 is calculated from the measured pressure drop and air permeance of the wooden section.

Figure 10 is an example comparing the calculated temperature profile with the measured values from November 26, 2009. Note that the data points are only measured at the material interfaces (see Figure 4). As can be seen from Figure 10, the heat flow is a combined convection-diffusion process. The higher the flow rate of the exfiltrating air, the more concave the curve will be, drifting the temperature profile across the wall into higher values.

Figure 11 is an example plotting the vapor pressure and corresponding saturation vapor pressure using data measured on January 10, 2010. The vapor pressure line in Figure 11 obeys an exponential law like the temperature line in Figure 10 due to airflow effects.

Figure 12 compares the predicted and measured rises in the moisture content of the fiberboard sheathing board specimen at

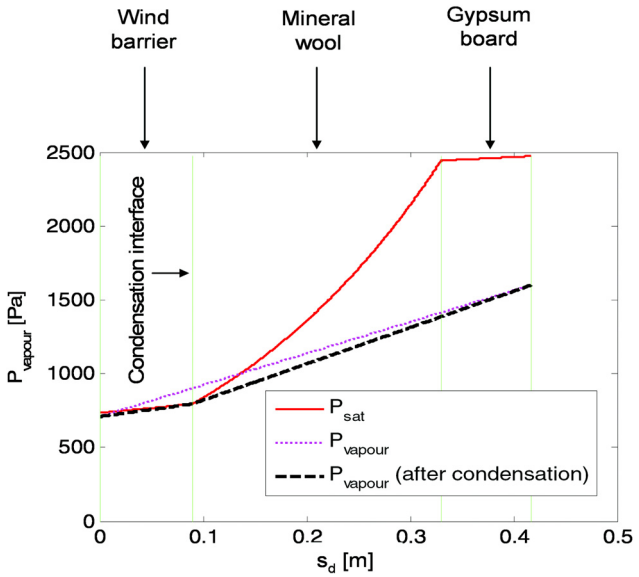

Figure 7 *A Glaser diagram for the gypsum section of the wall.*

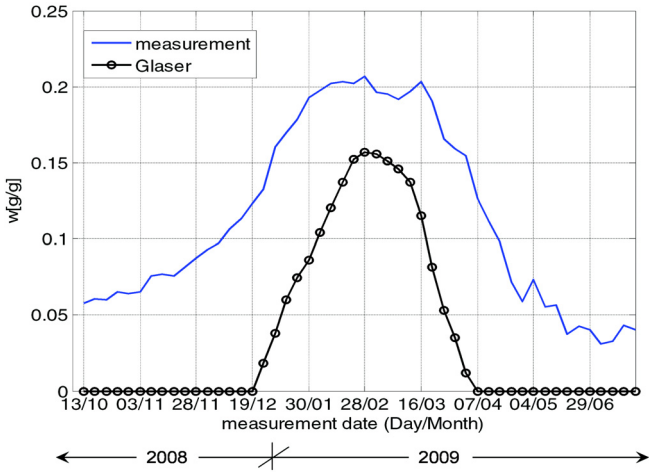

Figure 8 *Comparison between the measured moisture content and the Glaser model interstitial condensation prediction for the fiberboard sheathing specimen at the middle row of the gypsum section.*

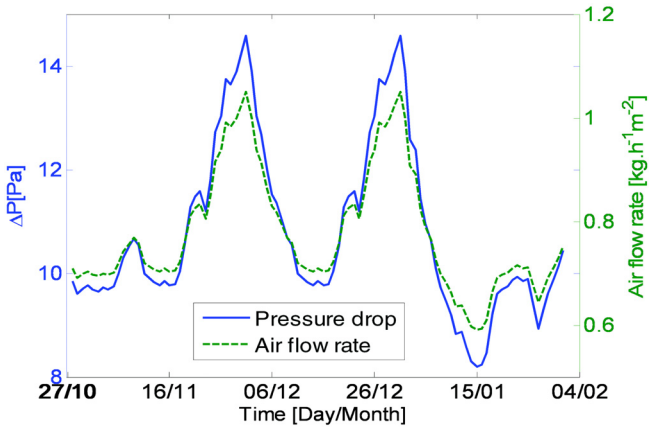

Figure 9 *Pressure drop and airflow rate across the test wall in the second winter period (mean value of the eight preceding days).*

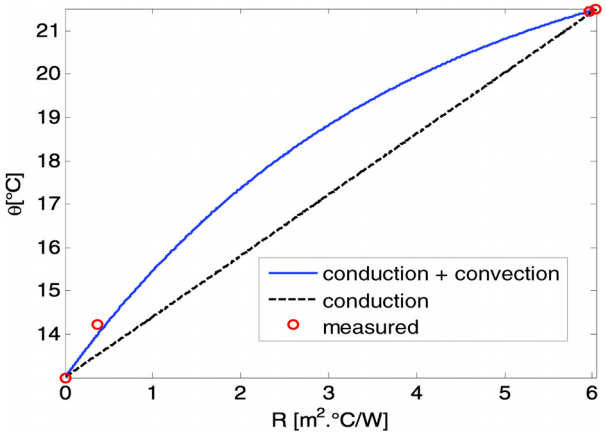

Figure 10 *Temperature profile (from outside to inside) across the wooden section of the wall on November 26, 2009.*

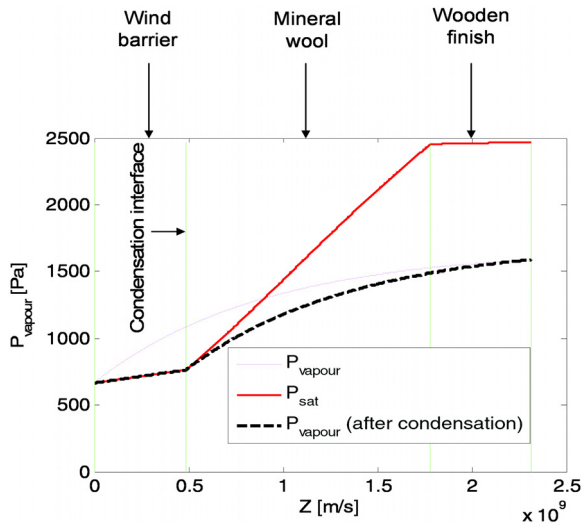

Figure 11 *Convection-diffusion vapor flow diagram for fiberboard sheathing specimen at the middle row of the wooden section on January 10th, 2010.*

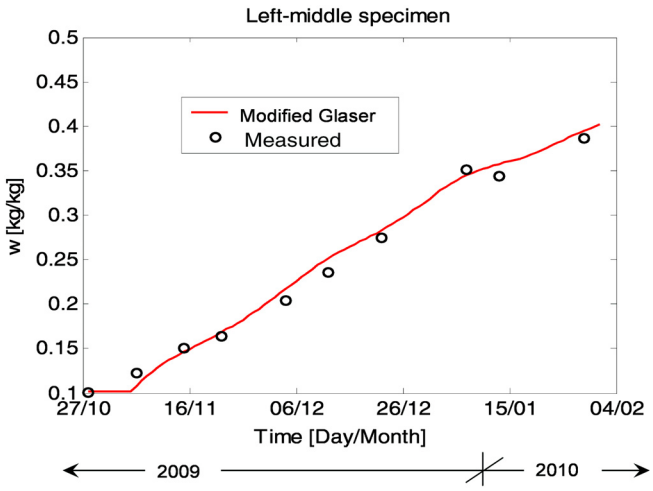

Figure 12 *Comparison of the modified Glaser model moisture content prediction against measurements for the fiberboard sheathing specimen at the middle row of the wooden section in the second winter period.*

the wooden section of the wall. The modified Glaser model predictions are in good agreement with the measurements.

The One-Dimensional Numerical Model

The one-dimensional numerical heat and moisture transport simulation is performed using the hygrothermal software Delphin 5.6.5 (Grunewald and Nicolai 2006). The modeling procedure comprises the descriptions of the fluxes in the calculation domain or in the field (between volume elements including material interfaces) and at the boundary (between volume elements and exterior or interior spaces) by physical models. Also included are models for storage processes such as adsorption, desorption, and release. The numerical solution is performed by semi-discretisation in space (using a finite/control volume method) and subsequent integration in time (Grunewald and Nicolai 2006).

The heat and moisture transfers through each section of the wall at the middle row of the test wall are simulated. For the entire simulation, a nonuniform grid system with unsteady-state mode is used. Measured building material properties, which are presented in Table 2, are the inputs of the model. A maximum time step of 30 s is set for time marching, and convergence criteria of moisture mass balance residual of 1E-6 kg/m^3 are used. Inside boundary conditions of temperature and humidity are taken from hourly measurements in the room, while outside conditions are the hourly measured ones in the outer cavity. The moisture contents of the fiberboard sheathing specimens are the output of the simulations.

Figure 13 shows a comparison of simulated and measured moisture contents of the fiberboard sheathing specimen at the middle row of a) the wooden section, b) the reference section, and c) the gypsum section; Figure 13d shows the used inside and outside vapor pressure boundary conditions.

The first-year moisture content prediction for the fiberboard sheathing specimen at the wooden section is rather good, but the simulation failed to track the measurement dynamics in the second winter when the interior finishing of the wooden section of the wall was drilled and convective forces influenced the transport mechanisms. The result is expected, since no air transport model is used in the simulation. In the second year, for the specimen at the reference section, the model discrepancy with the measurements is less than that for the specimen at the gypsum section. The reason the prediction error for the gypsum section is larger than that of the reference case could be that the interior finishing of the right part of the wall (gypsum board) is slightly air open, a phenomenon which is not considered in the model. In fact, in Figure 6, the airflow is also a cause for the difference in moisture contents of the fiberboard sheathing specimens located at the same section of the test wall but in different rows (top, middle, and bottom).

CONCLUSIONS

A test setup was built in the VLIET test building at the Laboratory of Building Physics of K.U. Leuven to analyze the hygrothermal behavior of lightweight building walls under real climatic conditions. The test wall was subdivided into three parts that differed in interior finishing. The wall was equipped with all necessary measurement sensors to follow the heat and moisture responses of the wall in detail. Furthermore, a bitumen-impregnated wood fiber board was used as a sheathing so that the amount of moisture accumulation could be measured by weighing a small specimen of the board. It was

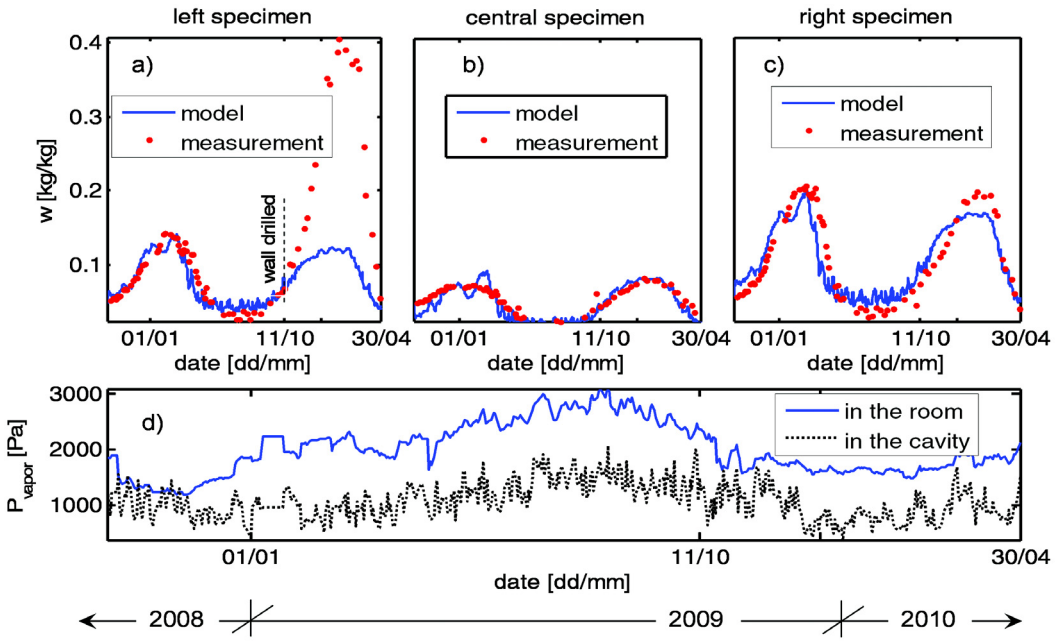

Figure 13 *Comparison of simulated and measured moisture content of the fiberboard sheathing specimen at the middle row of: a) at the wooden section, b) at the reference section, c) at the gypsum section, and d) shows the used inside and outside vapor pressure boundary conditions.*

found that as long as all walls were sufficiently airtight the amount of moisture accumulation was limited and the accumulated moisture in the winter period dried out in the summer for the given configuration. It was also found that the amount of moisture accumulation in the exterior sheathing is directly proportional to the vapor permeability of the interior finishing. As soon as the wooden section was made more air permeable, convective flow became the dominant cause of moisture buildup at the exterior sheathing of the section.

In addition to the measurements, some preliminary simulations have been performed. Primarily, the Glaser method is used to check the presence and quantify the amount of interstitial condensation in the wall. Bearing the assumptions and limitations of this simple calculation method in mind, fairly good results were obtained. In order to capture the flow dynamics in the drilled wooden section of the wall, a modified version of the Glaser model is used. The model predictions on the moisture gain of the fiberboard sheathing specimen at the wooden section were found to be in good agreement with the measured values. Finally, a one-dimensional numerical hygrothermal model was used to predict the moisture content response of the fiberboard sheathing specimens. As this model incorporates many more physical processes compared to the Glaser method, a better agreement between measurements and simulations was obtained. Since this preliminary simulation does not incorporate airflow effects, the moisture content predictions of the fiberboard sheathing specimen significantly deviate from measured values at the wooden section after the interior finishing of this part was drilled.

ACKNOWLEDGMENT

The results in this paper were obtained within the framework of the project IWT, SBO 050154, "Heat, air and moisture performance engineering: A whole building approach," funded by the Flemish Government. This financial support is gratefully acknowledged. We would also like to thank the Institute for Building Climatology at the Technical University of Dresden for providing the Delphine software.

NOMENCLATURE

k_{air}	=	air permeance, kg·m^{-2}·h^{-1}·Pa^{-1}
g_{air}	=	density of air flow rate, kg·m^{-2}·h^{-1}
Δp_{air}	=	air pressure difference, Pa
a	=	model parameters
b	=	model parameters
d	=	building material thickness, m
ρ	=	density, kg·m^{-3}
c_p	=	specific heat capacity at constant pressure, J·kg^{-1}·K^{-1}
λ	=	thermal conductivity, W·m^{-1}·K^{-1}
w	=	moisture content, kg·kg^{-1}
s_d	=	water vapor diffusion-equivalent air layer thickness, m
P_{vap}	=	vapor pressure
P_{sat}	=	saturation vapor pressure
Z	=	vapor diffusion resistance, m/s
θ	=	temperature, °C

REFERENCES

Abuku, M., B. Blocken, and S. Roels. 2009. Moisture response of building facades to wind-driven rain: Comparison of field measurements and numerical simulations. *Journal of Wind Engineering and Industrial Aerodynamics* 97(5-6):197–207.

Adan, O., H. Brocken, J. Carmeliet, H. Hens, S. Roels, and C.E. Hagentoft. 2004. Determination of liquid water transfer properties of porous building materials and development of numerical assessment methods: Introduction to the EC HAMSTAD project. *Journal of Thermal Envelope and Building Science* 27(4):253–60.

CEN. 2001. *ISO/CEN 13788, Hygrothermal performance of building components and building elements—Internal surface temperature to avoid critical surface humidity and interstitial condensation—Calculation methods.* Brussels: European Committee for Standardization.

Glaser, H. 1958. Temperatur und Dampfdruckverlauf in einer homogen Wand bei Feuchteausscheiding. *Kältetechnik*, pp. 174–81.

Grunewald, J. 1997. Diffusiver und konvektiver stoff- und energietransport in kapillarporösen baustoffen. PhD thesis, Institut für Bauklimatik, Technische Universität Dresden, Dresden, Germany.

Grunewald, J., and A. Nicolai. 2006. *CHAMPS-BES Program for Coupled Heat, Air Moisture and Pollutant Simulation in Building Envelope Systems, ver. 1, User Manual*. Dresden, Germany: Institut für Bauklimatik, Technische Universität Dresden.

Hagentoft, C.E., A.S. Kalagasidis, B. Adl-Zarrabi, S. Roels, J. Carmeliet, H. Hens, J. Grunewald, M. Funk, R. Becker, D. Shamir, O. Adan, H. Brocken, K. Kumaran, and R. Djebbar. 2004. Assessment method of numerical prediction models for combined heat, air and moisture transfer in building components. Benchmarks for one-dimensional cases. *Journal of Thermal Envelope and Building Science* 27(4):327–52.

Hens, H. 1975. Theoretische en experimentele studie van het hygrothermisch gedrag van bouw- en isolatiematerialen bij inwendige condensatie en droging, met toepassing op platte daken (in Dutch). PhD thesis, Department of Physics, K.U.Leuven, Leuven, Belgium.

Hens, H. 2007. *Building Physics—Heat, Air and Moisture: Fundamentals and Engineering Methods with Examples and Exercises*. Berlin: Ernst & Sohn.

ISO. 1991. *ISO 8302:1991, Thermal insulation—Determination of steady-state thermal resistance and related properties—Guarded hot plate apparatus*. Geneva: International Organization for Standardization.

ISO. 2000. *EN 12571:2000, Building materials; Determination of hygroscopic sorption curves*. Geneva: International Organization for Standardization.

ISO. 2001. *ISO 12572:2001, Hygrothermal performance of building materials and products—Determination of water vapour transmission properties*. Geneva: International Organization for Standardization.

Karagiozis, A. 1993. Overview of the 2D hygrothermal heat-moisture transport model LATENITE. Institute for Research in Construction, National Research Council, Canada.

Kumaran, K. 1996. Material properties. Final report, Vol. 3. Laboratorium Bouwfysica, Departement Burgerlijke Bouwkunde, KU Leuven, Belgium.

Künzel, H. 1994. Simultaneous heat and moisture transport in building components. One- and two-dimensional calculation using simple parameters. PhD thesis, Fraunhofer Institute of Building Physics, Universität Stuttgart, Germany.

Li, Q., J. Rao, and P. Fazio. 2009. Development of HAM tool for building envelope analysis. *Building and Environment* 44(5):1065–73.

Pedersen, C.R., 1990. Combined heat and moisture transfer in building constructions. PhD-thesis, Technical University of Denmark, Report no. 214.

Roels, S., C. James, P. Talukdar, and C.J. Simonson. 2009. Reliability of material data measurements for hygroscopic buffering. *ASHRAE Transactions* 115(2):111–25.

Roels, S., and M. Deurinck. 2010. The effect of a reflective underlay on the global thermal behaviour of pitched roofs. Submitted to *Building and Environment.*

Vos, B.H., and E.J.W. Coelman. 1967. Condensation in structures. Report no. BI-67-33/23, TNO-IBBC, Rijswijk, The Netherlands.